Research Article

Journal of Molecular Recognition

Received: 10 February 2011, Revised: 25 May 2011, Accepted: 25 May 2011, Published online in Wiley Online Library: 2011

(wileyonlinelibrary.com) DOI: 10.1002/jmr.1148

Structural and thermodynamic consequences of the replacement of zinc with environmental metals on estrogen receptor α–DNA interactions

Brian J. Deegan[a], Anna M. Bona[a], Vikas Bhat[a], David C. Mikles[a], Caleb B. McDonald[a], Kenneth L. Seldeen[a] and Amjad Farooq[a]*

Estrogen receptor α (ERα) acts as a transcription factor by virtue of the ability of its DNA-binding (DB) domain, comprised of a tandem pair of zinc fingers, to recognize the estrogen response element within the promoters of target genes. Herein, using an array of biophysical methods, we probe the structural consequences of the replacement of zinc within the DB domain of ERα with various environmental metals and their effects on the thermodynamics of binding to DNA. Our data reveal that whereas the DB domain reconstituted with divalent ions of zinc, cadmium, mercury, and cobalt binds to DNA with affinities in the nanomolar range, divalent ions of barium, copper, iron, lead, manganese, nickel, and tin are unable to regenerate DB domain with DNA-binding potential, although they can compete with zinc for coordinating the cysteine ligands within the zinc fingers. We also show that the metal-free DB domain is a homodimer in solution and that the binding of various metals only results in subtle secondary and tertiary structural changes, implying that metal coordination may only be essential for binding to DNA. Collectively, our findings provide mechanistic insights into how environmental metals may modulate the physiological function of a key nuclear receptor involved in mediating a plethora of cellular functions central to human health and disease. Copyright © 2011 John Wiley & Sons, Ltd.

Keywords: estrogen receptor α; zinc fingers; environmental metals; isothermal titration calorimetry; analytical light scattering; circular dichroism; steady-state fluorescence; steady-state absorbance

INTRODUCTION

Estrogen receptor α (ERα) is a member of a family of ligand-modulated transcription factors that have come to be known as nuclear receptors (NRs) (Evans, 1988; Thornton, 2001; Escriva *et al*., 2004; McKenna *et al*., 2009). ERα mediates the action of estrogens such as estradiol in a diverse array of cellular processes, and its hyperactivation leads to the genesis of large fractions of breast cancer (Heldring *et al*., 2007). ERα is constructed on a modular architecture, also shared by other members of the NR family, comprised of a central DNA-binding (DB) domain flanked between an N-terminal trans-activation (TA) domain and a C-terminal ligand-binding (LB) domain. Upon the binding of estrogens to the LB domain, ERα translocates to the nucleus and binds as a homodimer with a twofold axis of symmetry to the estrogen response element (ERE), containing the AGGTCAnnnTGACCT consensus sequence, located within the promoters of target genes (Klinge, 2001). Binding to DNA is accomplished through a pair of tandem C4-type zinc fingers located within the DB domain, with each finger containing a Zn^{2+} ion coordinated in a tetrahedral arrangement by four highly conserved cysteine residues to generate the $Zn^{2+}[Cys]_4$ metal–protein complex (Schwabe *et al*., 1990, 1993) (Figure 1). Importantly, while the first zinc finger (ZF-I) within each monomer of DB domain recognizes the hexanucleotide sequence 5′-AGGTCA-3′ within the major groove at each end of the ERE duplex, the second zinc finger (ZF-II) is responsible for the homodimerization of DB domain.

Upon binding to the promoters of target genes through its DB domain, the LB domain of ERα recruits a multitude of cellular proteins in an estrogen-dependent manner, such as transcription factors, co-activators, and co-repressors, to the site of DNA transcription, thereby allowing it to exert its action at the genomic level in a concerted fashion (Ham and Parker, 1989; Darimont *et al*., 1998). The TA domain is believed to be responsive to growth factors acting through mitogen-activated protein kinase signaling, and thus, it further synergizes the action of various co-activators and co-repressors recruited by the LB domain at the site of DNA transcription (Kato *et al*., 1995; Warnmark *et al*., 2003). In this

* *Correspondence to: A. Farooq, Department of Biochemistry and Molecular Biology and USylvester Braman Family Breast Cancer Institute, Leonard Miller School of Medicine, University of Miami, Miami, FL 33136, FL, USA.*
E-mail: amjad@farooqlab.net

a *B. J. Deegan, A. M. Bona, V. Bhat, D. C. Mikles, C. B. McDonald, K. L. Seldeen, A. Farooq*
Department of Biochemistry and Molecular Biology and USylvester Braman Family Breast Cancer Institute, Leonard Miller School of Medicine, University of Miami, Miami, FL 33136, USA

Abbreviations: *ALS, analytical light scattering; CD, circular dichroism; DB, DNA binding; DLS, dynamic light scattering; ERα, estrogen receptor α; ERE, estrogen response element; ITC, isothermal titration calorimetry; LB, ligand binding; NR, nuclear receptor; SEC, size-exclusion chromatography; SLS, static light scattering; SSA, steady-state absorbance; SSF, steady-state fluorescence; TA, trans-activation; ZF, zinc finger.*

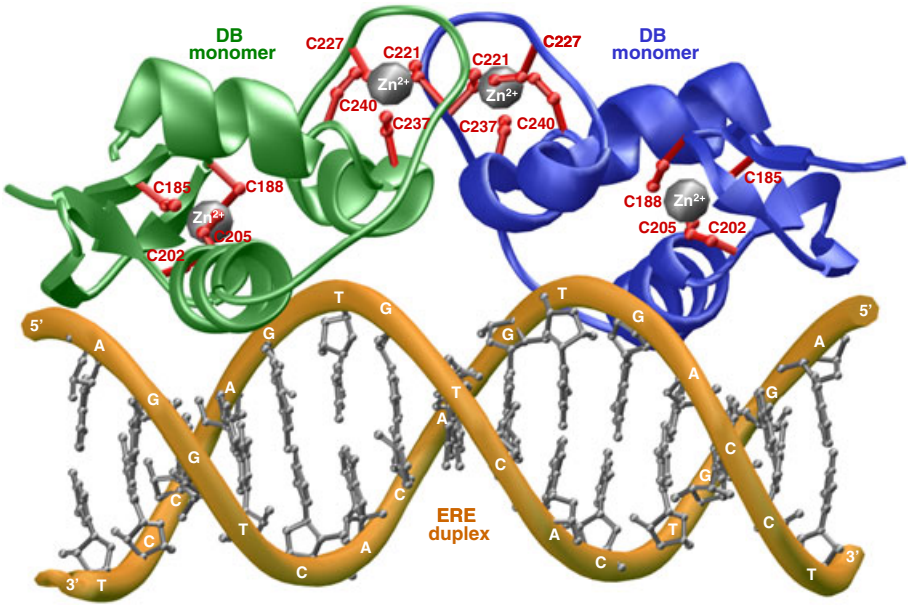

Figure 1. 3D structural model of the DNA-binding (DB) domain of human estrogen receptor α in complex with estrogen response element duplex containing the AGGTCAcagTGACCT consensus sequence based on the crystal structure (PDB# 1HCQ) determined by Rhodes and co-workers (Schwabe *et al*., 1993). The structural model was built as described earlier (Deegan *et al*., 2010) and rendered using RIBBONS (Carson, 1991). Note that the DB domain binds to DNA as a homodimer with a twofold axis of symmetry. One monomer of DB domain is shown in green and the other in blue. The Zn^{2+} divalent ions are depicted as gray spheres and the side chain moieties of cysteine residues being coordinated in red. The DNA backbone is shown in yellow, and the bases are colored gray for clarity.

manner, ERα and other NRs mediate a diverse array of cellular functions from embryonic development to metabolic homeostasis, and their aberrant function has been widely implicated in disease (Brzozowski *et al*., 1997; Gottlieb *et al*., 2004; Gurnell and Chatterjee, 2004; Noy, 2007; Sonoda *et al*., 2008; McEwan, 2009).

Discovered more than a quarter of century ago (Miller *et al*., 1985), the ZF is one of the most common motifs found in transcription factors (Green *et al*., 1998; Wolfe *et al*., 2000). Several lines of evidence suggest that metals other than zinc can serve as coordination sites for cysteine ligands within ZFs with important consequences on cellular processes involved in gene expression, DNA repair, and genomic stability (Freedman *et al*., 1988; Thiesen and Bach, 1991; Hartwig, 2001; Bal *et al*., 2003; Blessing *et al*., 2004; Kopera *et al*., 2004; Hartwig *et al*., 2010). In an effort to further our understanding of the interaction of metals with ZFs, we analyze here the structural consequences of the replacement of zinc within the DB domain of ERα with various environmental metals and their effects on the thermodynamics of binding to DNA using an array of biophysical methods. Our data reveal that whereas the DB domain reconstituted with divalent ions of zinc, cadmium, mercury, and cobalt binds to DNA with affinities in the nanomolar range, divalent ions of barium, copper, iron, lead, manganese, nickel, and tin are unable to regenerate DB domain with DB potential, although they can compete with zinc for coordinating the cysteine ligands within the ZFs. We also show that the metal-free DB domain is a homodimer in solution and that the binding of various metals only results in subtle secondary and tertiary structural changes, implying that metal coordination may only be essential for binding to DNA. Collectively, our findings provide mechanistic insights into how environmental metals may modulate the physiological function of a key NR involved in mediating a plethora of cellular functions central to human health and disease.

MATERIALS AND METHODS

Protein preparation

The DB domain (residues 176–250) of human ERα was cloned into pET101 bacterial expression vector with a C-terminal polyhistidine (His)-tag using Invitrogen TOPO technology (Invitrogen Carlsbad, California, USA). The recombinant protein was expressed in bacteria supplemented with 50 μM $ZnCl_2$ and purified to apparent homogeneity on a Ni-NTA affinity column followed by treatment on a Hiload Superdex 200 (GE Healthcare, Little Chalfont, UK) size-exclusion chromatography (SEC) column coupled in-line with GE Akta FPLC system (GE Healthcare, Little Chalfont, UK) as described previously (Deegan *et al*., 2010, 2011). Zinc divalent ions were stripped by the treatment of purified protein in Tris buffer (50 mM Tris, 200 mM NaCl, and 10 mM β-mercaptoethanol at pH 8.0) containing 8 M urea and 10 mM EDTA. After denaturation of protein overnight, EDTA was removed under denatured conditions by dialysis in acetate buffer (50 mM sodium acetate, 200 mM NaCl, and 10 mM β-mercaptoethanol at pH 6.0) containing 8 M urea. Further dialysis of protein in acetate buffer containing one of the metal chlorides at a final protein-to-metal molar ratio of 1:10 led to the simultaneous removal of urea and reconstitution of the DB domain with the corresponding metal divalent ions. It is important to note that the reconstitution of DB domain at pH 6.0 was necessary to prevent the formation of insoluble salts such as lead chloride. Additionally, acetate buffer was preferred over phosphate buffer because of the insolubility of various metal phosphates. Metal-reconstituted DB domain was extensively dialyzed in an appropriate buffer to remove excess metal ions. Protein concentration was determined by the fluorescence-based Quant-It assay (Invitrogen) and spectrophotometrically using an extinction

coefficient of 14 940 $M^{-1}cm^{-1}$. Results from both assays were in an excellent agreement.

DNA synthesis

21-mer DNA oligos containing the ERE consensus site AGGT CAnnnTGACCT were commercially obtained from Sigma Genosys (St. Louis, Missouri, USA). The complete nucleotide sequences of the sense and antisense oligos constituting the ERE duplex are 5′-cccAGGTCAcagTGACCTgcg-3′ and 3′-gggTCCAGTgtcACTG-GAcgc-5′.

Oligo concentrations were determined spectrophotometrically on the basis of their extinction coefficients derived from their nucleotide sequences. Sense and antisense oligos were annealed together to generate the ERE duplex as described earlier (Deegan *et al*., 2010, 2011).

Isothermal titration calorimetry measurements

Isothermal titration calorimetry (ITC) measurements were performed on a MicroCal VP-ITC instrument (MicroCal), and data were acquired and processed using fully automized features in MicroCal ORIGIN (MicroCal). All measurements were repeated at least three times. Briefly, protein and DNA samples were prepared in 50 mM sodium phosphate buffer containing 5 mM β-mercaptoethanol at pH 7.0 and de-gassed using the ThermoVac accessory (ThermoVac) for 5 min. The experiments were initiated by injecting 25 × 10-μl aliquots of 50–100 μM of ERE duplex from the syringe into the calorimetric cell containing 1.8 ml of 2–5 μM of DB domain of ERα reconstituted with various metals at 25°C. The change in thermal power as a function of each injection was automatically recorded using the ORIGIN software, and the raw data were further processed to yield binding isotherms of heat release per injection as a function of molar ratio of ERE duplex to dimer-equivalent DB domain. The heats of mixing and dilution were subtracted from the heat of binding per injection by carrying out a control experiment in which the same buffer in the calorimetric cell was titrated against the ERE duplex in an identical manner. Control experiments with scrambled dsDNA oligos generated similar thermal power to that obtained for the buffer alone, implying that there was no non-specific binding of DB domains to non-cognate DNA. To extract various thermodynamic parameters, the binding isotherms were iteratively fit to a built-in one-site model by non-linear least squares regression analysis using the ORIGIN software as described previously (Wiseman *et al*., 1989; Deegan *et al*., 2010).

Analytical light scattering experiments

Analytical light scattering (ALS) experiments were conducted on a Wyatt miniDAWN TREOS triple-angle static light scattering (SLS) detector and Wyatt QELS dynamic light scattering (DLS) detector coupled in-line with a Wyatt Optilab rEX differential refractive index detector (Wyatt, Santa Barbara, California, USA) and interfaced to a Hiload Superdex 200 SEC column under the control of a GE Akta FPLC system within a chromatography refrigerator at 10°C. The DB domain of ERα pre-treated with EDTA to strip divalent zinc ions and upon reconstitution with divalent ions of various metals was loaded onto the column at a flow rate of 1 ml min^{-1}, and the data were automatically acquired using the Astra software (Wyatt, Santa Barbara, California, USA). All protein samples were prepared in 50 mM sodium phosphate buffer containing 5 mM β-mercaptoethanol at pH 7.0, and the starting concentrations injected onto the column were between 20 and 50 μM. The angular and concentration dependence of SLS intensity of each protein species resolved in the flow mode was measured by the Wyatt miniDAWN TREOS detector. The SLS data were analyzed according to the following built-in Zimm equation in Astra software (Zimm, 1948; Wyatt, 1993):

$$(Kc/R_\theta) = ((1/M_{obs}) + 2A_2c)\left[1 + \left(\left(16\pi^2(R_g)^2/3\lambda^2\right)\sin^2(\theta/2)\right)\right] \quad (1)$$

where R_θ is the excess Rayleigh ratio due to protein in the solution as a function of protein concentration c (mg ml^{-1}) and the scattering angle θ (42°, 90°, and 138°), M_{obs} is the observed molecular mass of each protein species, A_2 is the second virial coefficient, λ is the wavelength of laser light in solution (658 nm), R_g is the radius of gyration of protein, and K is given by the following relationship:

$$K = [4\pi^2 n^2 (dn/dc)^2]/N_A\lambda^4 \quad (2)$$

where n is the refractive index of the solvent, dn/dc is the refractive index increment of the protein in solution, and N_A is the Avogadro's number (6.02×10^{23} mol^{-1}). If we assume that $c \rightarrow 0$ and $\theta \rightarrow 0$, then Equation (1) reduces to

$$(Kc/R_\theta) = 1/M_{obs} \quad (3)$$

Thus, under dilute protein concentrations ($c \rightarrow 0$) and at low scattering angles ($\theta \rightarrow 0$), the y-intercept of Equation (1) equates to $1/M_{obs}$. Accordingly, the weighted average value for M_{obs} was obtained from the y-intercept of linear fits of a range of (Kc/R_θ)–$\sin^2(\theta/2)$ plots as a function of protein concentration along the elution profile of each protein species using SLS measurements at three scattering angles. The time and concentration dependence of DLS intensity fluctuation of each protein species resolved in the flow mode was measured by the Wyatt QELS detector positioned at 90° with respect to the incident laser beam. The DLS data were iteratively fit using non-linear least squares regression analysis to the following built-in equation in the Astra software (Koppel, 1972; Berne and Pecora, 1976; Chu, 1991):

$$G(\tau) = \alpha \exp(-2\Gamma\tau) + \beta \quad (4)$$

where $G(\tau)$ is the autocorrelation function of DLS intensity fluctuation I, τ is the delay time of autocorrelation function, Γ is the decay rate constant of autocorrelation function, α is the initial amplitude of autocorrelation function at zero delay time, and β is the baseline offset (the value of autocorrelation function at infinite delay time). Thus, fitting the above equation to a range of $G(\tau)$–τ plots as a function of protein concentration along the elution profile of each protein species computes the average value of Γ using DLS measurements at a scattering angle of 90°. Accordingly, the translational diffusion coefficient (D_t) of each protein species was calculated from the following relationship:

$$D_t = \left[(\Gamma\lambda^2)/(16\pi^2 n^2 \sin^2(\theta/2))\right] \quad (5)$$

where λ is the wavelength of laser light in solution (658 nm), n is the refractive index of the solvent, and θ is the scattering angle

(90°). Additionally, the hydrodynamic radius (R_h) of each protein species was calculated from the Stokes–Einstein relationship:

$$R_h = [(k_B T)/(6\pi\eta D_t)] \quad (6)$$

where k_B is the Boltzman's constant (1.38×10^{-23} JK^{-1}), T is the absolute temperature, and η is the solvent viscosity. It should be noted that in both the SLS and DLS measurements, protein concentration (c) along the elution profile of each protein species was automatically quantified in the Astra software from the change in refractive index (Δn) with respect to the solvent as measured by the Wyatt Optilab rEX detector using the following relationship:

$$c = (\Delta n)/(dn/dc) \quad (7)$$

where dn/dc is the refractive index increment of the protein in solution.

Circular dichroism analysis

Circular dichroism (CD) analysis was conducted on a Bio-Logic (Claix, France) MOS450/SFM400 spectropolarimeter (Bio-Logic) thermostatically controlled with a water bath at 25°C, and data were acquired using the Biokine software (Bio-Logic, Claix, France). Briefly, experiments were conducted on 20–50 μM of DB domain of ERα pre-treated with EDTA to strip divalent zinc ions and upon reconstitution with divalent ions of various metals in 50 mM sodium phosphate buffer at pH 7.0. For far-UV measurements in the 190-nm to 250-nm wavelength range, experiments were conducted in a quartz cuvette with a 2-mm path length. For near-UV measurements in the 250-nm to 350-nm wavelength range, experiments were conducted in a quartz cuvette with a 10-mm path length. All data were recorded with a slit bandwidth of 2 nm at a scan rate of 3 nm min^{-1}. Data were normalized against reference spectra to remove the contribution of buffer. The reference spectra were obtained in a similar manner on a 50-mM sodium phosphate buffer at pH 7.0. Each data set represents an average of at least four scans acquired at 1-nm intervals. Data were converted to molar ellipticity, [θ], as a function of wavelength (λ) of electromagnetic radiation using the following equation:

$$[\theta] = \left[\left(10^5 \Delta\varepsilon\right)/cl\right] \text{deg cm}^2 \text{ dmol}^{-1} \quad (8)$$

where $\Delta\varepsilon$ is the observed ellipticity in mdeg, c is the protein concentration in μM, and l is the cuvette path length in centimeters. All data were processed and analyzed using the MicroCal ORIGIN software.

Steady-state absorbance experiments

Steady-state absorbance (SSA) spectra were collected on a Jasco V-630 spectrophotometer using a quartz cuvette with a 10-mm path length at 25°C. Briefly, experiments were conducted on 5 μM of DB domain of ERα pre-treated with EDTA to strip divalent zinc ions and upon reconstitution with divalent ions of various metals in a 50-mM sodium phosphate buffer at pH 7.0. All data were recorded in the 200-nm to 350-nm wavelength range using a 1.5-nm slit bandwidth. Data were normalized against reference spectra to remove the contribution of buffer. The reference spectra were obtained in a similar manner on a 50-mM sodium phosphate buffer at pH 7.0.

Steady-state fluorescence measurements

Steady-state fluorescence (SSF) spectra were collected on a Jasco FP-6300 spectrofluorometer (Jasco Easton, Maryland, USA) using a quartz cuvette with a 10-mm path length at 25°C. Briefly, experiments were conducted on 5 μM of DB domain of ERα pre-treated with EDTA to strip divalent zinc ions and upon reconstitution with divalent ions of various metals in 50-mM sodium phosphate buffer at pH 7.0. Excitation wavelength was 295 nm, and emission was acquired from 310 to 500 nm. All data were recorded using a 2.5-nm bandwidth for both excitation and emission. Data were normalized against reference spectra to remove the contribution of buffer. The reference spectra were obtained in a similar manner on a 50-mM sodium phosphate buffer at pH 7.0.

RESULTS AND DISCUSSION

Binding of the DNA-binding domain of ERα to DNA is restored upon substitution of zinc with only specific divalent metal ions

To determine the extent to which environmental metals may be able to replace zinc within the ZFs of ERα, we measured the binding of ERE duplex to the DB domain pre-treated with EDTA to remove divalent zinc ions (as a control) and upon reconstitution with divalent ions of various metals using ITC (Figure 2). Our data reveal that whereas the DB domain reconstituted with divalent ions of zinc, cadmium, mercury, and cobalt binds to DNA with affinities in the nanomolar range (Table 1), divalent ions of barium, copper, iron, lead, manganese, nickel, and tin are unable to regenerate DB domain with DB potential. These data are consistent with previous studies demonstrating that DB domain of ERα regenerated with divalent ions of zinc, cadmium, and cobalt binds DNA but not that regenerated with divalent ions of copper and nickel (Predki and Sarkar, 1992, 1994).

Although the replacement of zinc with cadmium, mercury, and cobalt restores binding to DNA with very similar affinities, the underlying thermodynamic forces display remarkable contrast (Table 1). Thus, whereas the binding of DB domain reconstituted with various metals is universally driven by favorable enthalpic changes accompanied by entropic penalty, the binding of DB domain reconstituted with cadmium and mercury results in the release of 5–15 kcal mol^{-1} of additional enthalpic contribution to the overall free energy relative to reconstitution with zinc and cobalt. We believe that such enthalpic advantage is due to the fact that the DB domain reconstituted with cadmium and mercury is only partially structured and that it only becomes fully structured upon binding to DNA in a binding-coupled folding manner. To shed further light on this phenomenon, we also measured heat capacity changes associated with the binding of various metal-coordinated DB domains to DNA (Figure 2 and Table 1). It has been previously reported that a large negative heat capacity change (ΔC_p) associated with protein–DNA interactions is indicative of protein folding coupled to binding of DNA (Spolar and Record, 1994). Remarkably, our analysis reveals that whereas a large negative ΔC_p indeed accompanies the binding of mercury-coordinated DB domain to DNA, ΔC_p associated with the binding of cadmium-coordinated DB domain is smaller than that observed for DB domain reconstituted with zinc and cobalt. In fact, ΔC_p accompanying the binding of cobalt-coordinated DB domain to DNA is similar to that observed for

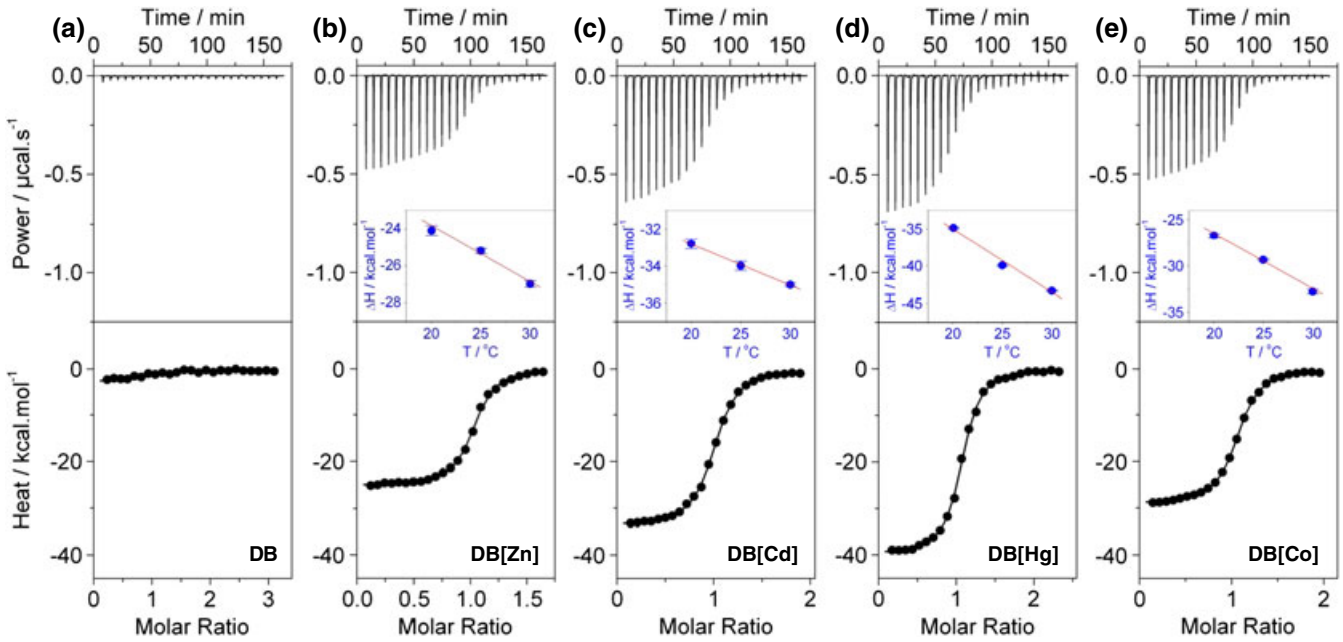

Figure 2. Representative isothermal titration calorimetry (ITC) isotherms for the binding of estrogen response element (ERE) duplex to the DNA-binding (DB) domain of estrogen receptor α pre-treated with EDTA to strip divalent zinc ions (a) and upon reconstitution with divalent ions of zinc (b), cadmium (c), mercury (d), and cobalt (e). The upper panels show the raw ITC data expressed as change in thermal power with respect to time over the period of titration. In the lower panels, change in molar heat is expressed as a function of molar ratio of ERE duplex to dimer-equivalent DB domain. The solid lines in the lower panels represent the fit of data to a one-site model, based on the binding of a ligand to a macromolecule assuming the law of mass action, using the ORIGIN software (Wiseman *et al*., 1989; Deegan *et al*., 2010). The insets in the top panels represent Δ*H*–*T* plots for the corresponding protein–DNA complexes. The solid line in red represents linear fit to the corresponding data.

mercury-coordinated DB domain. However, it is important to note that such discrepancies in the values of ΔC_p do not necessarily contradict the corresponding enthalpic contributions to the overall free energy of binding of various metal-coordinated DB domains to DNA. On the contrary, it is believed that factors other than protein folding can also contribute to ΔC_p. In particular, factors such as entrapment of water molecules and counterions within interfacial cavities as well as proton-linked equilibria during the formation of macromolecular complexes may also contribute to heat capacity changes (Cooper *et al*., 2001; Cooper, 2005). Thus, the large negative values of ΔC_p reported here may not solely reflect the folding of DB domain upon binding to DNA, but they could also arise from other factors. We have previously shown that the binding of DB domain of ERα to DNA

Table 1. Thermodynamic parameters obtained from isothermal titration calorimetry (ITC) measurements at 25 °C for the binding of estrogen response element (ERE) duplex to the DNA-binding (DB) domain of estrogen receptor α pre-treated with EDTA to strip divalent zinc ions (DB) and upon reconstitution with divalent ions of zinc (DB[Zn]), cadmium (DB[Cd]), mercury (DB[Hg]), and cobalt (DB[Co])

	K_d (nM)	ΔH (kcal mol^{-1})	$T\Delta S$ (kcal mol^{-1})	ΔG (kcal mol^{-1})	ΔC_p (kcal mol^{-1} K^{-1})
DB	NB	NB	NB	NB	NB
DB[Zn]	68 ± 8	−25.20 ± 0.15	−15.40 ± 0.21	−9.80 ± 0.07	−0.28 ± 0.04
DB[Cd]	69 ± 5	−33.99 ± 0.25	−24.20 ± 0.20	−9.78 ± 0.04	−0.22 ± 0.04
DB[Hg]	59 ± 4	−39.95 ± 0.13	−30.07 ± 0.16	−9.88 ± 0.04	−0.85 ± 0.01
DB[Co]	81 ± 2	−29.35 ± 0.10	−19.66 ± 0.10	−9.69 ± 0.01	−0.60 ± 0.01

The values for the affinity (K_d) and enthalpy change (ΔH) accompanying the binding of ERE duplex to the DB domain reconstituted with various metals were obtained from the fit of a one-site model, based on the binding of a ligand to a macromolecule using the law of mass action, to the corresponding ITC isotherms as described earlier (Wiseman *et al*., 1989; Deegan *et al*., 2010). Free energy of binding (ΔG) was calculated from the relationship $\Delta G = RT\ln K_d$, where R is the universal molar gas constant (1.99 cal mol^{-1} K^{-1}) and T is the absolute temperature (K). Entropic contribution ($T\Delta S$) to binding was calculated from the relationship $T\Delta S = \Delta H - \Delta G$. Heat capacity change ($\Delta C_p$) was calculated from the slope of Δ*H*–*T* plot for the corresponding protein–DNA complex (Figure 2). Binding stoichiometries generally agreed to within ±10%. Errors were calculated from at least three independent measurements. All errors are given to one standard deviation. Note that the DB domain pre-treated with EDTA to strip divalent zinc ions and upon reconstitution with divalent metal ions of barium, copper, iron, lead, manganese, nickel, and tin showed no binding (NB) to the ERE duplex.

is coupled to proton uptake (Deegan *et al.*, 2010). Interestingly, this phenomenon is not affected by the replacement of zinc with divalent ions of cadmium, mercury, and cobalt. As shown in Figure 3, the observed enthalpies for the binding of various metal-reconstituted DB domains to DNA are strongly dependent on buffer, implying that binding to DNA is coupled to proton uptake irrespective of the nature of metal coordination. Our analysis also suggests that the binding of metal-reconstituted DB domains to DNA involves a net uptake of two protons in agreement with our previous study (Deegan *et al.*, 2010).

Importantly, the metal coordination of cysteine ligands in a tetrahedral arrangement to generate the $M^{2+}[Cys]_4$ metal–protein complex may be important for the proper folding of the DB domain such that it can recognize the ERE duplex in a specific manner. This is further corroborated by the knowledge that the divalent ions of zinc, cadmium, mercury, and cobalt are all capable of coordinating their ligands with tetrahedral geometries (Rulisek and Vondrasek, 1998). However, the fact that divalent ions of metals such as nickel and manganese can also adopt tetrahedral geometry implies that the factors other than coordination geometry may also hold key to determining whether a particular divalent metal ion can replace zinc within the ZFs of the DB domain. Of particular importance are the ionic radii and internuclear coordination distances of various divalent metal ions in complex with their ligands. Interestingly, the ionic radii of hydrated divalent ions of all divalent metal ions analyzed here fall in the 100-pm to 150-pm range (Marcus, 1988), and there seems to be no correlation between their ionic radii and their ability to replace zinc within the ZFs of the DB domain. To what extent the hydration shell, or the extent to which a divalent metal ion becomes hydrated in solution, may be an important determinant of its ability to coordinate a given ligand also remains debatable. In short, it is not clear from our studies as to why some divalent ions can replace zinc within the ZFs of the DB domain while others cannot on the basis of their physicochemical properties such as coordination geometry, ionic radius, and internuclear coordination distance. Our study, thus, clearly warrants further investigation of the precise mechanisms driving protein–metal interactions.

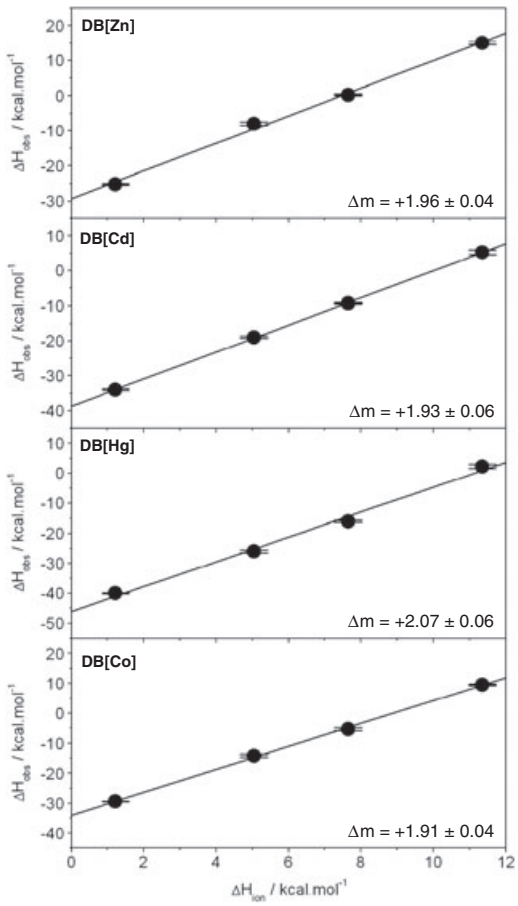

Figure 3. Dependence of observed enthalpy (ΔH_{obs}) as a function of ionization enthalpy (ΔH_{ion}) of various buffers upon the binding of estrogen response element duplex to the DNA-binding (DB) domain of estrogen receptor α reconstituted with divalent ions of zinc (DB[Zn]), cadmium (DB[Cd]), mercury (DB[Hg]), and cobalt (DB[Co]). The ΔH_{ion} of various buffers used were +1.22 kcal mol^{-1} (phosphate), +5.02 kcal mol^{-1} (HEPES), +7.64 kcal mol^{-1} (Ticine), and +11.35 kcal mol^{-1} (Tris) (Fukada and Takahashi, 1998; Kozlov and Lohman, 2000; Ortiz-Salmeron *et al.*, 2001). The solid lines within each panel represent linear fits to data points, and the net change in the number of protons (Δm) uptaken per DB monomer upon binding to DNA was calculated from the corresponding slopes as described earlier (Deegan *et al.*, 2010). Error bars were calculated from at least three independent measurements. All errors are given to one standard deviation.

Substitution of zinc with other divalent metal ions does not affect hydrodynamic properties of the DNA-binding domain of estrogen receptor α

To further investigate how the substitution of zinc with cadmium, mercury, and cobalt affects the hydrodynamic properties of the DB domain of ERα, we conducted ALS analysis based on the first principles of hydrodynamics with no assumptions (Figure 4). It is generally believed that the DB domain is monomeric in solution and that it only homodimerizes upon binding to DNA (Schwabe *et al.*, 1990, 1993). Contrary to this school of thought, our analysis reveals that the DB domain predominantly exists as a homodimer in solution even in the absence of DNA (Table 2). Analysis on a non-reducing sodium dodecyl sulfate–polyacrylamide gel electrophoresis further confirmed that the ability of DB domain to homodimerize in solution was not an artifact of intermolecular disulfide bridges.

Strikingly, the DB domain not only homodimerizes in the absence of DNA, but even the metal coordination does not appear to be obligatory. Thus, the metal-free DB domain not only appears to behave as a homodimer in solution in a manner akin to when reconstituted with divalent metal ions but its hydrodynamic radius also does not seem to change, implying that the protein possesses a globular fold even in the absence of metal coordination. It is however important to note that our ALS measurements were conducted on DB domains in the 20-μM to 50-μM range. Although all DB domains behaved as homodimers within this concentration range, it is conceivable that the DB domain in the absence or presence of metal coordination may behave as a monomer at protein concentrations in the submicromolar range. It should, however, be noted that ALS measurements for the DB domain outside the 20-μM to 50-μM concentration range were not feasible. Thus, whereas the ALS signal-to-noise ratio starts to get poorer at protein concentrations below 20 μM making hydrodynamic analysis less reliable, the DB domain appears to precipitate on the SEC column at concentrations above 50 μM. Although it has not been possible at this stage, our future efforts will further explore the ability of DB domain to homodimerize in solution using alternative methodologies such as analytical ultracentrifugation

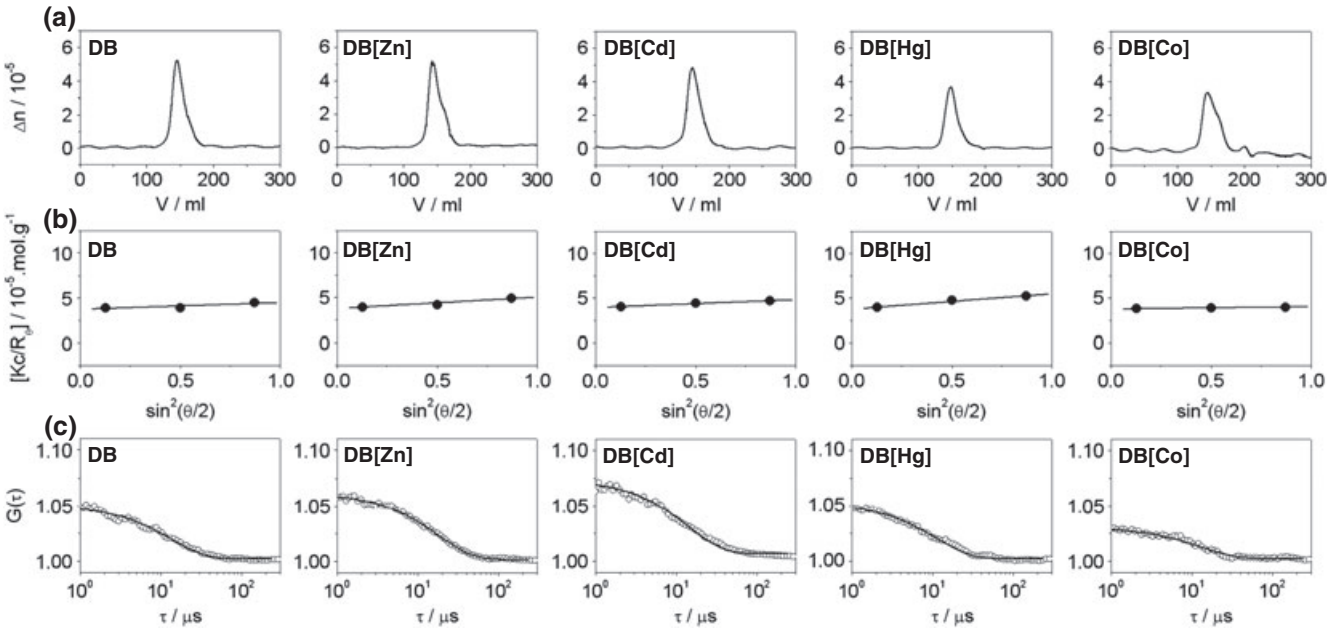

Figure 4. Representative analytical light scattering chromatograms for the DNA-binding (DB) domain of estrogen receptor α pre-treated with EDTA to strip divalent zinc ions (DB) and upon reconstitution with divalent ions of zinc (DB[Zn]), cadmium (DB[Cd]), mercury (DB[Hg]), and cobalt (DB[Co]). (a) Elution profiles as monitored by the differential refractive index (Δn) plotted as a function of elution volume (V) for the indicated species. (b) Partial Zimm plots obtained from analytical static light scattering measurements at a specific protein concentration for indicated species. The solid lines through the data points represent linear fits. (c) Autocorrelation function plots obtained from analytical dynamic light scattering measurements at a specific protein concentration for the indicated species. The solid lines through the data points represent non-linear least squares fits to Equation (4).

and native mass spectrometry. Nonetheless, these observations suggest strongly that the DB domain may be able to attain a globular fold alone and that metal coordination may only be essential for binding to DNA. Importantly, these findings are consistent with the knowledge that the LB domain of ERα also behaves as a homodimer in solution (Brandt and Vickery, 1997), suggesting that both the LB and DB domains contribute to the dimerization of ERα in solution (Notides and Nielsen, 1974; Notides *et al*., 1981).

Table 2. Hydrodynamic parameters obtained from analytical light scattering measurements for the DNA-binding (DB) domain of estrogen receptor α pre-treated with EDTA to strip divalent zinc ions (DB) and upon reconstitution with divalent ions of zinc (DB[Zn]), cadmium (DB[Cd]), mercury (DB[Hg]), and cobalt (DB[Co])

	M_{obs} (kD)	D_t (μm²sec⁻¹)	R_h (Å)	Associativity
DB	26±1	102±3	24±1	Dimer
DB[Zn]	27±1	104±9	23±2	Dimer
DB[Cd]	26±1	102±5	25±1	Dimer
DB[Hg]	27±1	103±4	23±1	Dimer
DB[Co]	26±1	108±5	23±1	Dimer

M_{obs}, D_t, and R_h are, respectively, the observed molecular mass, translational diffusion coefficient, and hydrodynamic radius for each indicated species. Note that the calculated molecular mass of the recombinant DB domain from amino acid sequence alone is 13 kD. Errors were calculated from at least three independent measurements. All errors are given to one standard deviation.

Substitution of zinc with other divalent metal ions results in subtle secondary and tertiary structural changes within the DNA-binding domain of estrogen receptor α

To further understand how the binding of various metals changes secondary and tertiary structural features of the DB domain of ERα, we conducted a CD analysis of DB domain in complex with various divalent metal ions (Figure 5). Consistent with our ALS analysis above, the metal-free DB domain indeed displays spectral features in the far-UV region characteristic of a mixed αβ-fold, with bands centered around 210 and 220 nm (Figure 5(a)). The metal-free DB domain also displays near-UV spectral features characteristic of a globular fold with bands centered around 260 and 280 nm (Figure 5(b)), due respectively to Phe and Trp/Tyr residues. Upon the addition of divalent ions of zinc and cobalt, the far-UV and near-UV spectra of the DB domain undergo sharp enhancement in intensity, implying that the binding of zinc and cobalt induces substantial folding of the protein. In contrast, addition of cadmium results in only slight changes in the spectral intensities of the DB domain in the far-UV and near UV-regions, suggesting that cadmium coordination also results in some degree of folding but is not sufficient to lead to fully structured protein. Strikingly, in the presence of mercury, the far-UV and near-UV spectral intensities of the DB domain undergo slight reduction. This salient observation implies that the coordination of mercury has little or no effect on the secondary or tertiary structure of the DB domain in agreement with our thermodynamic data (Table 1). We believe that this is most likely due to the preference of mercury to coordinate its ligands with linear geometry (Rulisek and Vondrasek, 1998). Accordingly, the cysteine ligands within the DB domain may be coordinated by mercury with a linear geometry as opposed to tetrahedral arrangement necessary for its proper folding as

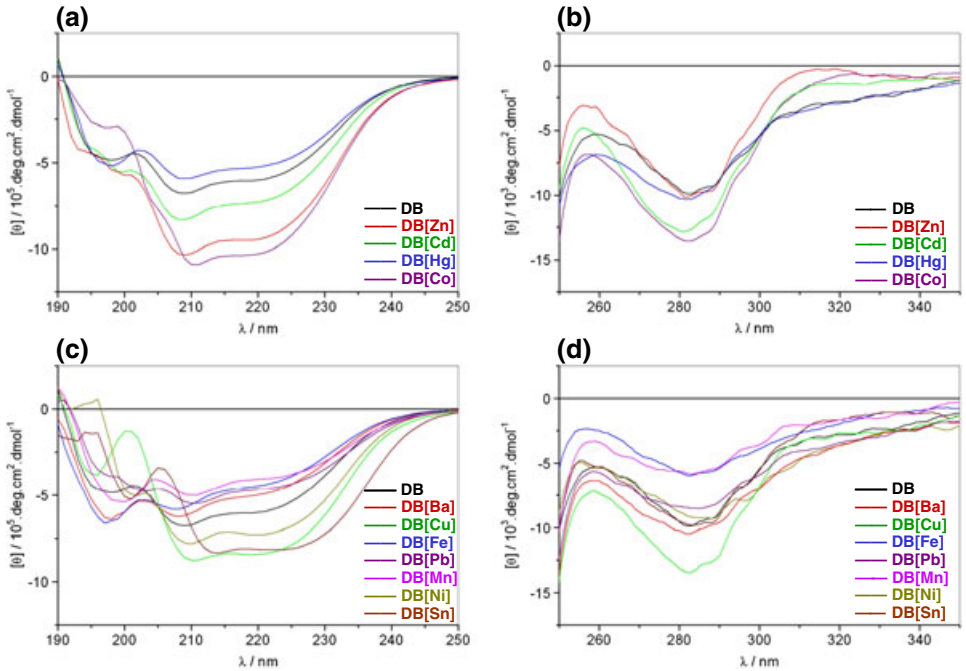

Figure 5. Representative far-UV circular dichroism (CD) spectra in (a) and (c) and near-UV CD spectra in (b) and (d) for the DNA-binding (DB) domain of estrogen receptor α pre-treated with EDTA to strip divalent zinc ions (DB) and upon reconstitution with divalent ions of zinc (DB[Zn]), cadmium (DB[Cd]), mercury (DB[Hg]), cobalt (DB[Co]), barium (DB[Ba]), copper (DB[Cu]), iron (DB[Fe]), lead (DB[Pb]), manganese (DB[Mn]), nickel (DB[Ni]), and tin (DB[Sn]). Note that the spectra with divalent metal ions that can regenerate the DB domain with DNA-binding potential are presented in (a) and (b), whereas the spectra for divalent metal ions that fail to do so are in (c) and (d).

observed in the case of coordination with zinc, cobalt, and cadmium divalent ions. In light of our thermodynamic data (Table 1), it is conceivable that the binding of DNA causes mercury to switch its coordination from linear to tetrahedral geometry so as to allow the DB domain to undergo proper folding necessary for DNA recognition.

Taken together, our CD data are consistent with the notion that the DB domain may be able to attain a globular fold alone and that metal coordination may only be essential for binding to DNA. It should also be noted here that the failure of DB domain regenerated with divalent ions of barium, copper, iron, lead, manganese, nickel, and tin to bind DNA does not necessarily imply failure to replace zinc within the ZFs of the DB domain. Indeed, it has been previously reported that the divalent ions of copper can replace zinc within the ZFs of DB and that such substitution is met with profound effects on the physiological action of ERα (Young *et al*., 1977; Fishman and Fishman, 1988; Hutchens *et al*., 1992; Predki and Sarkar, 1992). It is thus conceivable that divalent ions of barium, copper, iron, lead, manganese, nickel, and tin can replace zinc within the ZFs of DB domain, but their inability to coordinate cysteine ligands in a tetrahedral arrangement results in improper folding such that the DB domain can no longer recognize the target DNA. This is indeed further supported by our CD measurements of DB domain in complex with divalent metal ions of barium, copper, iron, lead, manganese, nickel, and tin (Figure 5(c), (d)). Evidently, the addition of these metal divalent ions results in marked changes in both the secondary and tertiary structural features of the DB domain, implying that these metals can also coordinate the protein but in a non-productive manner. In light of these observations, we believe that metals such as barium, copper, iron, lead, manganese, nickel, and tin may also be able to compete with zinc for coordinating to the DB domain within living cells with important consequences on the physiological action of ERα.

DNA-binding domain of estrogen receptor α reconstituted with various metals displays distinct spectroscopic properties

In an attempt to further analyze how reconstitution of DB domain of ERα with various divalent metal ions results in structural changes, we also measured SSA and SSF spectra (Figure 6(a), (b)). As expected, the metal-free DB domain displays characteristic absorbance spectral features in the UV region with maxima centered around 225 and 280 nm (Figure 6(a)), due respectively to peptide bonds and Trp/Tyr/Phe residues. Additionally, the DB domain reconstituted with various metals also displays similar spectroscopic features, but the spectral intensity of the 280-nm band appears to undergo reduction, implying that metal-binding most likely induces structural changes within the DB domain, due for example to burial of Trp/Tyr/Phe residues. Such metal-mediated modulation of spectral features is further indicative of specific metal–protein interactions as noted previously (Bal *et al*., 2003; Kopera *et al*., 2004). Consistent with our absorbance measurements, the DB domain reconstituted with various metals also displays fluorescence properties distinct from those observed for the metal-free DB domain (Figure 6(b)). Thus, the increase in fluorescence intensity and the emission wavelength maximum (λ_{max}) undergoing a slight blueshift in the DB domain reconstituted with various metals relative to metal-free DB domain is indicative of the transfer of Trp to a more hydrophobic environment, thereby suggesting that the protein undergoes conformational changes upon metal coordination.

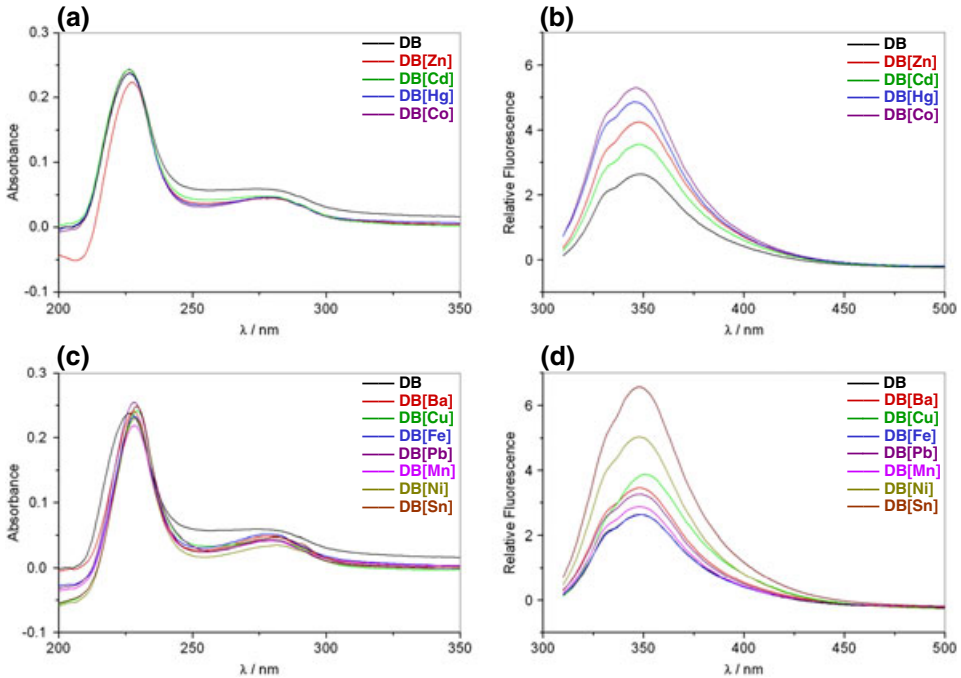

Figure 6. Representative steady-state absorbance spectra in (a) and (c) and steady-state fluorescence spectra in (b) and (d) for the DNA-binding (DB) domain of estrogen receptor α pre-treated with EDTA to strip divalent zinc ions (DB) and upon reconstitution with divalent ions of zinc (DB[Zn]), cadmium (DB[Cd]), mercury (DB[Hg]), cobalt (DB[Co]), barium (DB[Ba]), copper (DB[Cu]), iron (DB[Fe]), lead (DB[Pb]), manganese (DB[Mn]), nickel (DB[Ni]), and tin (DB[Sn]). Note that the spectra with divalent metal ions that can regenerate the DB domain with DNA-binding potential are presented in (a) and (b), whereas the spectra for divalent metal ions that fail to do so are in (c) and (d).

Interestingly, mercury-coordinated DB domain also undergoes substantial enhancement in fluorescence, implying that coordination of mercury also results in structural changes within the DB domain. However, this observation is at odds with our CD data above, wherein the CD spectral features of mercury-coordinated DB domain did not differ much from those observed for the metal-free DB domain. It is however conceivable that mercury coordination of cysteine ligands within the DB domain with Cys–Hg^{2+}–Cys linear geometry primarily results in perturbation of environment around Trp, which could also account for the enhancement of fluorescence observed here. Notably, our SSA and SSF measurements also suggest that the addition of divalent ions of barium, copper, iron, lead, manganese, nickel, and tin also results in changes in spectroscopic properties of DB domain (Figure 6(c) and (d)), implying that although these metals cannot regenerate DB domain with DB potential, they are nonetheless capable of competing with zinc for the ZFs in agreement with our CD data.

CONCLUSIONS

In the industrialized world, the environment has come to play an increasing role on human health because of the presence of obnoxious chemicals in a wide variety of sources. In particular, over the past decade or so, it has become clear that metal ions absorbed from various environmental sources can potentiate the transcriptional activity of ERα within the body leading to the development and progression of breast cancer (Garcia-Morales *et al*., 1994; Martin *et al*., 2003; Darbre, 2006). Although it is generally believed that such metals up-regulate ERα by virtue of their ability to mimic the action of endogenous estrogens, our data presented here suggest that some of these metals may also be able to replace zinc within the ZFs of the DB domain and thereby modulate its binding to the promoters of target genes (Klinge, 2001). In particular, our data suggest that metals such as barium, copper, iron, lead, manganese, nickel, and tin may coordinate to cysteine ligands within the DB domain in a manner that it can no longer bind to DNA. It is thus quite possible that these metals may influence the physiological action of ERα by virtue of their ability to compete with zinc for coordinating to DB domain although their concentration is likely to be much lower than zinc within living cells. More importantly, given that the hyperactivation of ERα is linked to the genesis of large fractions of breast cancer (Deroo and Korach, 2006; Heldring *et al*., 2007), deciphering the molecular basis of how environmental metals modulate the transcriptional activity of ERα bears the potential to not only expand our biomedical knowledge but may also lead to the development of novel anti-cancer therapies harboring greater efficacy coupled with low toxicity. Toward this goal, our present study provides mechanistic insights into how environmental metals may replace zinc within the ZFs of ERα and thus bears important consequences on understanding its physiological function in human health and disease.

ACKNOWLEDGEMENTS

This work was supported by funds from the National Institutes of Health (Grant no. R01-GM083897) and the USylvester Braman Family Breast Cancer Institute to A.F. C.B.M. is a recipient of a postdoctoral fellowship from the National Institutes of Health (Award no. T32-CA119929). B.J.D. and A.F. are members of the Sheila and David Fuente Graduate Program in Cancer Biology at the Sylvester Comprehensive Cancer Center of the University of Miami.

REFERENCES

Bal W, Schwerdtle T, Hartwig A. 2003. Mechanism of nickel assault on the zinc finger of DNA repair protein XPA. *Chem. Res. Toxicol.* **16**: 242–248.

Berne BJ, Pecora R (1976). Dynamic light scattering (New York, Wiley).

Blessing H, Kraus S, Heindl P, Bal W, Hartwig A. 2004. Interaction of selenium compounds with zinc finger proteins involved in DNA repair. *Eur. J. Biochem.* **271**: 3190–3199.

Brandt ME, Vickery LE. 1997. Cooperativity and dimerization of recombinant human estrogen receptor hormone-binding domain. *J. Biol. Chem.* **272**: 4843–4849.

Brzozowski AM, Pike AC, Dauter Z, Hubbard RE, Bonn T, Engstrom O, Ohman L, Greene GL, Gustafsson JA, Carlquist M. 1997. Molecular basis of agonism and antagonism in the oestrogen receptor. *Nature* **389**: 753–758.

Carson M 1991. Ribbons 2.0. *J. Appl. Crystallogr.* **24**: 958–961.

Chu B (1991). Laser light scattering: basic principles and practice (Boston, Academic).

Cooper A 2005. Heat capacity effects in protein folding and ligand binding: a re-evaluation of the role of water in biomolecular thermodynamics. *Biophys. Chem.* **115**: 89–97.

Cooper A, Johnson CM, Lakey JH, Nollmann M. 2001. Heat does not come in different colours: entropy–enthalpy compensation, free energy windows, quantum confinement, pressure perturbation calorimetry, solvation and the multiple causes of heat capacity effects in biomolecular interactions. *Biophys. Chem.* **93**: 215–230.

Darbre PD. 2006. Metalloestrogens: an emerging class of inorganic xenoestrogens with potential to add to the oestrogenic burden of the human breast. *J. Appl. Toxicol.* **26**: 191–197.

Darimont BD, Wagner RL, Apriletti JW, Stallcup MR, Kushner PJ, Baxter JD, Fletterick RJ, Yamamoto KR. 1998. Structure and specificity of nuclear receptor–coactivator interactions. *Genes Dev.* **12**: 3343–3356.

Deegan BJ, Seldeen KL, McDonald CB, Bhat V, Farooq A. 2010. Binding of the ERalpha nuclear receptor to DNA is coupled to proton uptake. *Biochemistry* **49**: 5978–5988.

Deegan BJ, Bhat V, Seldeen KL, McDonald CB, Farooq A 2011. Genetic variations within the ERE motif modulate plasticity and energetics of binding of DNA to the ERalpha nuclear receptor. *Arch. Biochem. Biophys.*; In Press.

Deroo BJ, Korach KS. 2006. Estrogen receptors and human disease. *J. Clin. Invest.* **116**: 561–570.

Escriva H, Bertrand S, Laudet V. 2004. The evolution of the nuclear receptor superfamily. *Essays Biochem.* **40**: 11–26.

Evans RM. 1988. The steroid and thyroid hormone receptor superfamily. *Science* **240**: 889–895.

Fishman JH, Fishman J. 1988. Copper and endogenous mediators of estradiol action. *Biochem. Biophys. Res. Commun.* **152**: 783–788.

Freedman LP, Luisi BF, Korszun ZR, Basavappa R, Sigler PB, Yamamoto KR. 1988. The function and structure of the metal coordination sites within the glucocorticoid receptor DNA binding domain. *Nature* **334**: 543–546.

Fukada H, Takahashi K 1998. Enthalpy and heat capacity changes for the proton dissociation of various buffer components in 0.1 M potassium chloride. *Proteins* **33**: 159–166.

Garcia-Morales P, Saceda M, Kenney N, Kim N, Salomon DS, Gottardis MM, Solomon HB, Sholler PF, Jordan VC, Martin MB. 1994. Effect of cadmium on estrogen receptor levels and estrogen-induced responses in human breast cancer cells. *J. Biol. Chem.* **269**: 16896–16901.

Gottlieb B, Beitel LK, Wu J, Elhaji YA, Trifiro M. 2004. Nuclear receptors and disease: androgen receptor. *Essays Biochem.* **40**: 121–136.

Green A, Parker M, Conte D, Sarkar B. 1998. Zinc finger proteins: a bridge between transition metals and gene regulation. *J. Trace Elem. Exp. Med.* **11**: 103–118.

Gurnell M, Chatterjee VK. 2004. Nuclear receptors in disease: thyroid receptor beta, peroxisome-proliferator-activated receptor gamma and orphan receptors. *Essays Biochem.* **40**: 169–189.

Ham J, Parker MG. 1989. Regulation of gene expression by nuclear hormone receptors. *Curr. Opin. Cell Biol.* **1**: 503–511.

Hartwig A 2001. Zinc finger proteins as potential targets for toxic metal ions: differential effects on structure and function. *Antioxid. Redox Signal.* **3**: 625–634.

Hartwig A, Schwerdtle T, Bal W. 2010. Biophysical analysis of the interaction of toxic metal ions and oxidants with the zinc finger domain of XPA. *Methods Mol. Biol.* **649**: 399–410.

Heldring N, Pike A, Andersson S, Matthews J, Cheng G, Hartman J, Tujague M, Strom A, Treuter E, Warner M, Gustafsson JA. 2007. Estrogen receptors: how do they signal and what are their targets. *Physiol. Rev.* **87**: 905–931.

Hutchens TW, Allen MH, Li CM, Yip TT 1992. Occupancy of a C2-C2 type 'zinc-finger' protein domain by copper. Direct observation by electrospray ionization mass spectrometry. *FEBS Lett.* **309**: 170–174.

Kato S, Endoh H, Masuhiro Y, Kitamoto T, Uchiyama S, Sasaki H, Masushige S, Gotoh Y, Nishida E, Kawashima H, *et al*. 1995. Activation of the estrogen receptor through phosphorylation by mitogen-activated protein kinase. *Science* **270**: 1491–1494.

Klinge CM. 2001. Estrogen receptor interaction with estrogen response elements. *Nucleic Acids Res.* **29**: 2905–2919.

Kopera E, Schwerdtle T, Hartwig A, Bal W. 2004. Co(II) and Cd(II) substitute for Zn(II) in the zinc finger derived from the DNA repair protein XPA, demonstrating a variety of potential mechanisms of toxicity. *Chem. Res. Toxicol.* **17**: 1452–1458.

Koppel DE. 1972. Analysis of macromolecular polydispersity in intensity correlation spectroscopy. *J. Chem. Phys.* **57**: 4814–4820.

Kozlov AG, Lohman TM. 2000. Large contributions of coupled protonation equilibria to the observed enthalpy and heat capacity changes for ssDNA binding to *Escherichia coli* SSB protein. *Proteins* **Suppl 4**: 8–22.

Marcus Y 1988. Ionic radii in aqueous solutions. *Chem. Rev.* **88**: 1475–1498.

Martin MB, Reiter R, Pham T, Avellanet YR, Camara J, Lahm M, Pentecost E, Pratap K, Gilmore BA, Divekar S, *et al*. 2003. Estrogen-like activity of metals in MCF-7 breast cancer cells. *Endocrinology* **144**: 2425–2436.

McEwan IJ. 2009. Nuclear receptors: one big family. *Methods Mol. Biol.* **505**: 3–18.

McKenna NJ, Cooney AJ, DeMayo FJ, Downes M, Glass CK, Lanz RB, Lazar MA, Mangelsdorf DJ, Moore DD, Qin J, *et al*. 2009. Minireview: evolution of NURSA, the Nuclear Receptor Signaling Atlas. *Mol. Endocrinol.* **23**: 740–746.

Miller J, McLachlan AD, Klug A. 1985. Repetitive zinc-binding domains in the protein transcription factor IIIA from *Xenopus* oocytes. *EMBO J.* **4**: 1609–1614.

Notides AC, Nielsen S. 1974. The molecular mechanism of the in vitro 4 S to 5 S transformation of the uterine estrogen receptor. *J. Biol. Chem.* **249**: 1866–1873.

Notides AC, Lerner N, Hamilton DE. 1981. Positive cooperativity of the estrogen receptor. *Proc. Natl. Acad. Sci. U. S. A.* **78**: 4926–4930.

Noy N 2007. Ligand specificity of nuclear hormone receptors: sifting through promiscuity. *Biochemistry* **46**: 13461–13467.

Ortiz-Salmeron E, Yassin Z, Clemente-Jimenez MJ, Las Heras-Vazquez FJ, Rodriguez-Vico F, Baron C, Garcia-Fuentes L. 2001. Thermodynamic analysis of the binding of glutathione to glutathione S-transferase over a range of temperatures. *Eur. J. Biochem.* **268**: 4307–4314.

Predki PF, Sarkar B. 1992. Effect of replacement of "zinc finger" zinc on estrogen receptor DNA interactions. *J. Biol. Chem.* **267**: 5842–5846.

Predki PF, Sarkar B. 1994. Metal replacement in "zinc finger" and its effect on DNA binding. *Environ. Health Perspect.* **102** Suppl 3: 195–198.

Rulisek L, Vondrasek J. 1998. Coordination geometries of selected transition metal ions (Co^{2+}, Ni^{2+}, Cu^{2+}, Zn^{2+}, Cd^{2+}, and Hg^{2+}) in metalloproteins. *J. Inorg. Biochem.* **71**; 115–127.

Schwabe JW, Neuhaus D, Rhodes D. 1990. Solution structure of the DNA-binding domain of the oestrogen receptor. *Nature* **348**: 458–461.

Schwabe JW, Chapman L, Finch JT, Rhodes D. 1993. The crystal structure of the estrogen receptor DNA-binding domain bound to DNA: how receptors discriminate between their response elements. *Cell* **75**: 567–578.

Sonoda J, Pei L, Evans RM. 2008. Nuclear receptors: decoding metabolic disease. *FEBS Lett.* **582**: 2–9.

Spolar RS, Record MT, Jr. 1994. Coupling of local folding to site-specific binding of proteins to DNA. *Science* **263**: 777–784.

Thiesen HJ, Bach C. 1991. Transition metals modulate DNA-protein interactions of SP1 zinc finger domains with its cognate target site. *Biochem. Biophys. Res. Commun.* **176**: 551–557.

Thornton JW. 2001. Evolution of vertebrate steroid receptors from an ancestral estrogen receptor by ligand exploitation and serial genome expansions. *Proc. Natl. Acad. Sci. U. S. A.* **98**: 5671–5676.

Warnmark A, Treuter E, Wright AP, Gustafsson JA. 2003. Activation functions 1 and 2 of nuclear receptors: molecular strategies for transcriptional activation. *Mol. Endocrinol.* **17**: 1901–1909.

Wiseman T, Williston S, Brandts JF, Lin LN. 1989. Rapid measurement of binding constants and heats of binding using a new titration calorimeter. *Anal. Biochem.* **179**: 131–137.

Wolfe SA, Nekludova L, Pabo CO. 2000. DNA recognition by Cys_2His_2 zinc finger proteins. *Annu. Rev. Biophys. Biomol. Struct.* **29**: 183–212.

Wyatt PJ. 1993. Light scattering and the absolute characterization of macromolecules. *Anal. Chim. Acta* **272**: 1–40.

Young PC, Cleary RE, Ragan WD. 1977. Effect of metal ions on the binding of 17beta-estradiol to human endometrial cytosol. *Fertil. Steril.* **28**: 459–463.

Zimm BH. 1948. The scattering of light and the radial distribution function of high polymer solutions. *J. Chem. Phys.* **16**: 1093–1099.

